

Different cell cycle modifications repress apoptosis at different steps independent of developmental signaling in *Drosophila*

Suozhi Qi and Brian R. Calvi*

Department of Biology, Indiana University, Bloomington, IN 47405

ABSTRACT Apoptotic cell death is important for the normal development of a variety of organisms. Apoptosis is also a response to DNA damage and an important barrier to oncogenesis. The apoptotic response to DNA damage is dampened in specific cell types during development. Developmental signaling pathways can repress apoptosis, and reduced cell proliferation also correlates with a lower apoptotic response. However, because developmental signaling regulates both cell proliferation and apoptosis, the relative contribution of cell division to the apoptotic response has been hard to discern *in vivo*. Here we use *Drosophila* oogenesis as an *in vivo* model system to determine the extent to which cell proliferation influences the apoptotic response to DNA damage. We find that different types of cell cycle modifications are sufficient to repress the apoptotic response to ionizing radiation independent of developmental signaling. The step(s) at which the apoptosis pathway was repressed depended on the type of cell cycle modification—either upstream or downstream of expression of the p53-regulated proapoptotic genes. Our findings have important implications for understanding the coordination of cell proliferation with the apoptotic response in development and disease, including cancer and the tissue-specific responses to radiation therapy.

Monitoring Editor

Orna Cohen-Fix
National Institutes of Health

Received: Mar 3, 2016

Revised: Apr 8, 2016

Accepted: Apr 8, 2016

INTRODUCTION

Genomic DNA is frequently damaged by mutagens and errors in DNA replication. Cell cycle checkpoints sense DNA damage, arrest the cell cycle, and activate DNA repair pathways (Weinert and Hartwell, 1993; Ciccio and Elledge, 2010). If genotoxic stress is severe, however, cells can either withdraw from the cell cycle or activate a programmed cell death (PCD). A major type of PCD is apoptosis, during which cells shrink as caspases and DNA endonucleases digest cellular contents (Fuchs and Steller, 2011). A defect in the

apoptotic response is a hallmark of cancer, underscoring the importance of apoptosis to prevent cells with multiple mutations from becoming oncogenic (Hanahan and Weinberg, 2011). Much remains unknown, however, about how cell proliferation and programmed cell death are normally balanced and integrated in the context of development and tissue homeostasis. In this study, we use *Drosophila* as model system to investigate how modifications to the cell cycle alter the apoptotic response to genotoxic stress *in vivo*.

Apoptosis is an important part of the normal development of a wide variety of plants and animals (Fuchs and Steller, 2011). Apoptosis can also be triggered by cell stress, including DNA damage. The fraction of cells that apoptose in response to DNA damage differs among tissues and times of development (Arya and White, 2015). In *Drosophila*, for example, cells in specific regions of the larval wing and eye imaginal disk apoptose infrequently after ionizing radiation (IR), revealing that there can be differences in apoptotic response even within a given tissue type (Moon *et al.*, 2005, 2006, 2008; Fan and Bergmann, 2008). In both mammals and flies, cell-specific differences in the apoptotic response are due, in part, to repression of p53-dependent and p53-independent apoptosis by developmental signaling pathways (Moon *et al.*, 2006, 2008; Jackson *et al.*, 2011; Arya and White, 2015). Another property that correlates with reduced apoptotic response is cell cycle arrest

This article was published online ahead of print in MBoC in Press (<http://www.molbiolcell.org/cgi/doi/10.1091/mbc.E16-03-0139>) on April 13, 2016.

*Address correspondence to: Brian R. Calvi (bcalvi@indiana.edu).

Abbreviations used: ATM, ataxia telangiectasia mutated; ATR, ataxia telangiectasia and Rad3 related; BrdU, bromodeoxyuridine; CDK1, cyclin-dependent kinase 1; DIAP, *Drosophila* inhibitor of apoptosis; FUCCI, fluorescent ubiquitination-based cell cycle indicator; GFP, green fluorescent protein; iEC, induced endocycling cells; IR, irradiation; PCD, programmed cell death; PFC, polar follicle cell; PH3, phospho-histone H3; TUNEL, terminal deoxynucleotidyl transferase dUTP nick end labeling.

© 2016 Qi and Calvi. This article is distributed by The American Society for Cell Biology under license from the author(s). Two months after publication it is available to the public under an Attribution–Noncommercial–Share Alike 3.0 Unported Creative Commons License (<http://creativecommons.org/licenses/by-nc-sa/3.0/>).

“ASCB,” “The American Society for Cell Biology,” and “Molecular Biology of the Cell” are registered trademarks of The American Society for Cell Biology.

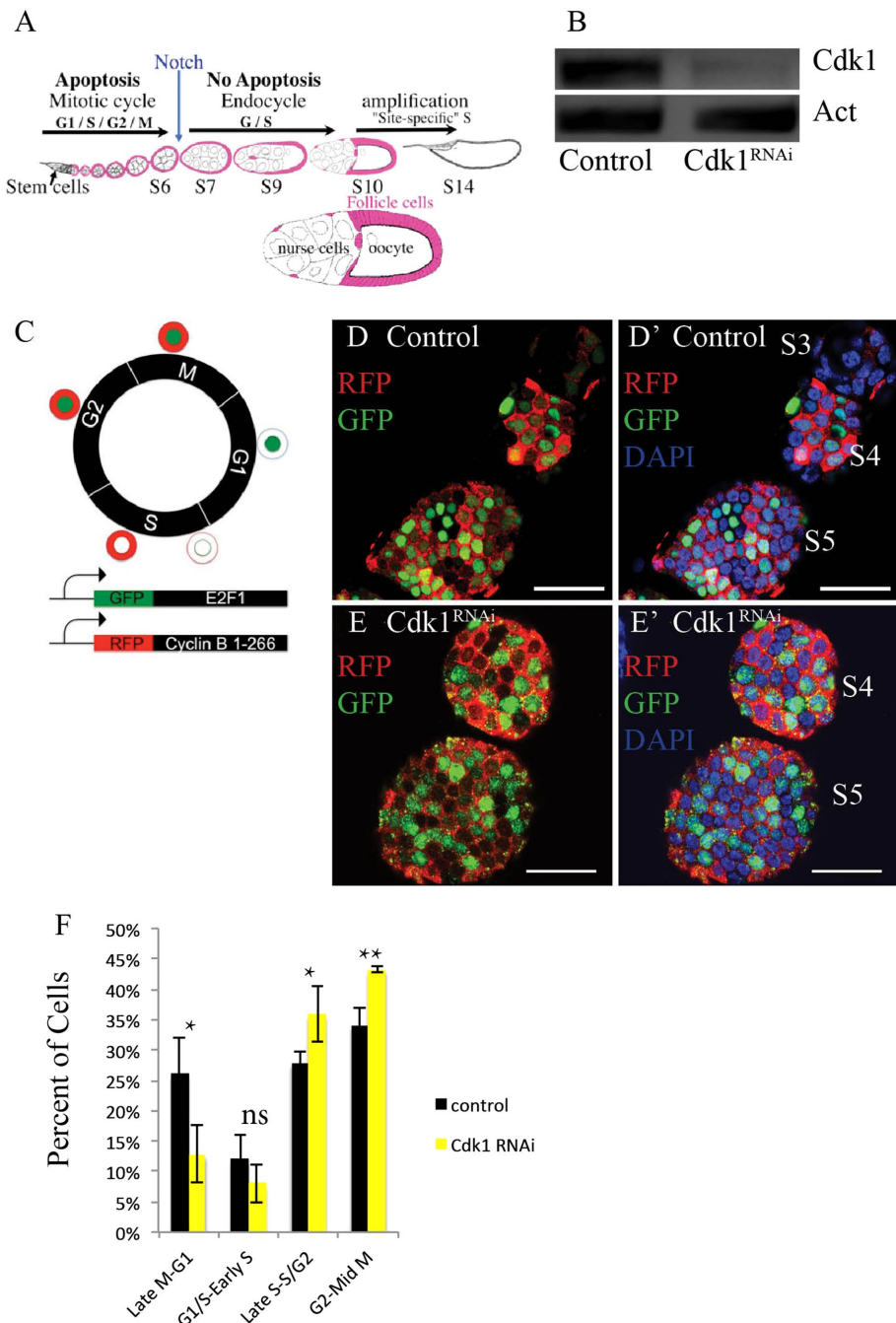


FIGURE 1: *Cdk1* knockdown alters cell cycle phasing in mitotic follicle cells. (A) Ovarian follicle cell cycles. One *Drosophila* ovariole (top) and one stage 10 egg chamber (bottom). Egg chambers are composed of one oocyte and 15 nurse cells surrounded by an epithelial sheet of somatic follicle cells (pink). Egg chambers mature through 14 stages as they migrate down the ovariole (to the right). Follicle cells mitotically proliferate during stages 1–6, switch to G/S endocycles in response to Notch signaling at stage 6/7, and then begin selective rereplication of genes required for eggshell synthesis (amplification) after stage 10B. Follicle cells that are mitotic cycling during stages 1–6 undergo caspase-dependent apoptosis in response to DNA damage, whereas endocycling or amplifying follicle cells during stages 7–14 do not. (B) RT-PCR of actin and *Cdk1* mRNA in *UAS-GFP^{RNAi}/+*; *hsp70-Gal4/+* and *hsp70-Gal4/UAS-Cdk1^{RNAi}* larvae after heat induction. (C) The *Drosophila* FUCCI system (Zielke *et al.*, 2014). RFP is fused to a Cyclin B degron, localized to the cytoplasm, and degraded from late M until early S phase. GFP is fused to an E2F1 degron, localized to the nucleus, and degraded during S phase. Cell cycle phasing is determined by the different combinations of red and green fluorescence, as shown in the cell cycle schematic. (D, D') FUCCI pattern in control mitotic cycling follicle cells. RFP and GFP double labeling (D) and triple labeling with DAPI (D') in stage 3–5 egg chambers from an *UAS-FUCCI*; *hsp70Gal4* female after heat induction. (E, E') FUCCI pattern in *Cdk1*-knockdown

(Spear and Glucksmann, 1941; Baldwin and Salthouse, 1959; Jackson *et al.*, 2011). For example, regions of the *Drosophila* eye and wing imaginal disks that do not apoptose readily correspond to groups of cells that are developmentally arrested in their cell cycle (Johnston and Edgar, 1998; Moon *et al.*, 2005; Tanaka-Matakatsu *et al.*, 2009). However, because developmental signaling regulates both cell proliferation and apoptotic pathways, it has been difficult to evaluate the relative contribution of cell cycle arrest to apoptotic repression in vivo.

We previously found that *Drosophila* cells in a variant cell cycle called the endocycle do not apoptose in response to genotoxic stress (Mehrotra *et al.*, 2008; Hassel *et al.*, 2014; Zhang *et al.*, 2014). Endocycles are composed of alternating G and S phases without mitosis and result in large, polyploid cells (Calvi, 2013; Fox and Duronio, 2013; Leslie, 2014). Cells switch from canonical mitotic cycles to endocycles as part of the normal development of a wide array of organisms, including humans (Fox and Duronio, 2013). Endocycling cells in multiple tissues of *Drosophila* do not apoptose in response to replication stress or IR (Mehrotra *et al.*, 2008; Hassel *et al.*, 2014; Zhang *et al.*, 2014). In endocycling larval salivary gland cells, apoptosis is repressed in at least two ways: tissue-specific proteolysis of the *Drosophila* orthologue of the p53 tumor suppressor and chromatin silencing of its proapoptotic target genes (Zhang *et al.*, 2014). These findings support the notion that a developmental switch to endocycles is associated with an active repression of the apoptotic response to DNA damage.

Our previous analysis of *Drosophila* ovarian follicle cells further suggested that there is a relationship between endocycles and the repression of apoptosis (Figure 1A; Mehrotra *et al.*, 2008; Hassel *et al.*, 2014). The somatic follicle cells form an epithelial sheet around the germline nurse cells and oocyte and undergo stereotypical transitions

follicle cells. RFP and GFP double labeling (E) and triple labeling with DAPI (E') in stage 4/5 egg chambers from a *UAS-FUCCI*; *hsp70Gal4/UAS-Cdk1^{RNAi}* female after heat induction. The images in D–E' are confocal sections of epithelial follicle cells on one surface of the egg chambers. Scale bars, 20 μ m. (F) Quantification of follicle cells in different cell cycle phases in S1–S6 egg chambers in the control or *Cdk1^{RNAi}* group based on FUCCI fluorescence. Mean percentages and SDs. Three biological replicates, >200 follicle cells/replicate, * $p < 0.05$ and ** $p < 0.01$ by unpaired t test.

in their cell cycle in strict coordination with maturation of the egg chamber as it migrates down an ovariole (Figure 1A). Follicle cells proliferate through a canonical mitotic cell cycle during stages 1–6 of oogenesis, they switch to an endocycle (G/S) at the stage 6/7 transition, and then in stage 10B, they begin to selectively rereplicate genes required for eggshell synthesis, a process called developmental gene amplification (Spradling, 1993; Calvi, 2006; Klusza and Deng, 2011; Hudson and Cooley, 2014). We showed that follicle cells in the mitotic cell cycle apoptose in response to replication stress or IR, whereas endocycling and amplification-stage follicle cells do not (Mehrotra et al., 2008). Follicle cells that are induced to precociously switch to endocycles before stage 7 through genetic ablation of mitosis also repressed apoptosis (Hassel et al., 2014). The repression of apoptosis in these induced endocycling cells (iECs) indicated that a switch to endocycles is sufficient to repress apoptosis. These results suggested a link between cell cycle and apoptotic programs. It remains unclear, however, what the nature of that link is and whether other types of cell cycle modification alter the apoptotic response independent of developmental signals.

In this study, we further investigate how modifications to the cell cycle influence the apoptotic response to DNA damage, using the *Drosophila* ovary as an in vivo model system. We find that arresting cells at different phases of the mitotic cell cycle also compromises the apoptotic response independent of developmental signaling. Of importance, different types of cell cycle modulation repressed apoptosis either upstream or downstream of the expression of p53-regulated proapoptotic genes, suggesting that multiple mechanisms link cell cycle and apoptosis. We discuss the important broader relevance of our data to interpreting how cell cycle modifications alter the apoptotic response in development and cancer.

RESULTS

Partial knockdown of CDK1 arrests follicle cell cycles and represses apoptosis

To investigate further the relationship between cell cycle programs and apoptotic competence, our strategy was to perturb the cell cycle in different ways and evaluate whether it coordinately induced endocycles and repressed apoptosis. We first knocked down *Cyclin-dependent kinase 1 (Cdk1)*, which is activated by dimerization with Cyclin A or B and required for mitosis. To do this, we used fly strains with a Gal4-inducible *UAS-Cdk1^{RNAi}* hairpin RNA (Ni et al., 2009). Heat induction of *UAS-Cdk1^{RNAi}* in larvae using an *hsp70-Gal4* driver significantly reduced but did not eliminate *Cdk1* mRNA (Figure 1B). To evaluate the effect of *Cdk1* knockdown on cell cycle progression, we used the recently created fluorescent ubiquitination-based cell cycle indicator (FUCCI) fly strains, which permit fluorescent detection of different cell cycle phases (Figure 1, C and D; Sakaue-Sawano et al., 2008; Zielke et al., 2014). We used a heat-inducible *hsp70-GAL4* to express *UAS-Cdk1^{RNAi}* in follicle cells in the FUCCI strain background and then analyzed the effect on cell cycle phasing of mitotic cycling follicle cells before stage 6. *Cdk1* knockdown significantly increased the number of cells in both late S–G2 and G2–early M phase (~80% of total) and decreased the number in G1-S phase (~20% of total) cells, indicating that *Cdk1* knockdown altered the cell cycle phasing of follicle cells (Figure 1, D–F).

Limitations of the FUCCI analysis are that it cannot distinguish between G2 and early M phase and also does not indicate whether cells are arrested or continuing to cycle with altered phasing. Therefore we further investigated the effect of *Cdk1* knockdown on follicle cell cycles using anti-phospho-histone H3 (PH3) to detect mitosis and incorporation of the nucleotide analogue bromodeoxyuridine (BrdU) for 1 h in vitro to detect S phase (Hendzel et al., 1997; Calvi

and Lilly, 2004). We compared the results with sibling *hsp70-GAL4; UAS-Cdk1^{RNAi}* females that were not heat treated and also with heat-treated *hsp70-GAL4; UAS-GFP^{RNAi}* females that expressed a negative control hairpin RNA against green fluorescent protein (GFP; Figure 2A and Supplemental Figure S1, A–F). RNA interference (RNAi) knockdown of *Cdk1* resulted in a large decrease in the number of BrdU-labeled cells, from ~25% in controls to <2% in the *Cdk1* knockdown (Figure 2, A, B, and D). In contrast, the fraction of follicle cells labeled with PH3 greatly increased, from ~4% in controls to ~50% in the *Cdk1* knockdown (Figure 2, A, B, and D). These cells had only diffuse PH3 labeling of partially condensed chromosomes, with no evidence for metaphase, anaphase, or telophase chromosomal configurations (Figure 2, C–C'). Many cells had a single focus of intense PH3 labeling that corresponded to the heterochromatic chromocenter, a genomic region that is phosphorylated first as cells enter mitosis, suggesting that these cells are arrested in early prophase (Hendzel et al., 1997). The large reduction in BrdU and increase in PH3 labeling suggested that *Cdk1* knockdown arrests follicle cell cycles.

To examine further the effect of *Cdk1* knockdown on cell cycle progression, we knocked down *Cdk1* in clones using the FLP-On recombination system (Pignoni and Zipursky, 1997). We marked cells by flipping on expression of *UAS-RFP* together with either *UAS-Cdk1^{RNAi}* or control *UAS-GFP^{RNAi}* and then examined the proliferation of these cells in clones (Pignoni and Zipursky, 1997). Cells within *GFP^{RNAi}* control clones proliferated to an average of 20 red fluorescent protein (RFP)-positive cells 4 d after induction, whereas the *Cdk1^{RNAi}* clones had an average of only two cells (Figure 2, E–G). This result suggests that *Cdk1* knockdown induces a cell cycle arrest within one or two cell divisions. There was no increase in nuclear size or 4',6-diamidino-2-phenylindole (DAPI) fluorescence in any of the cells, suggesting that *Cdk1* knockdown did not induce a switch to endocycles (Figure 2F). It is likely that the mitotic cell cycle arrest caused by *Cdk1* RNAi is a result of partial knockdown of CDK1 function because null mutations of *Cdk1* and *Cyclin A* or *Cyclin A* RNAi knockdown all induce a switch to endocycles (Sauer et al., 1995; Hayashi, 1996; Mihaylov et al., 2002; Hassel et al., 2014). Taken together, these results suggest that *Cdk1* RNAi knockdown results in a cell cycle arrest, with most cells arresting in G2 to early M phase.

We next evaluated whether *Cdk1* knockdown altered the apoptotic response to DNA damage. After knockdown of *Cdk1* with RNAi, adult females were irradiated with 40 Gy of γ -rays. Cell death was assayed by terminal deoxynucleotidyl transferase dUTP nick end labeling (TUNEL) 4 h after IR, a time when p53-dependent apoptosis predominates (Gavrieli et al., 1992; Brodsky et al., 2000; Ollmann et al., 2000). In control ovaries, IR resulted in an increase in TUNEL-positive mitotic cycling follicle cells, from <1 to ~10% (Figure 3, A, B, and E). Knockdown of *Cdk1* reduced the fraction of TUNEL-positive cells after IR by an order of magnitude to ~1%, a frequency not significantly different from that for unirradiated controls (Figure 3, C–E). Apoptosis was also significantly lower in *Cdk1* knockdown cells 24 h after IR, a time when delayed p53-independent apoptosis is active (~2 vs. ~14% in control siblings; Wichmann et al., 2006). Heat-induced expression of *GFP^{RNAi}* had no effect on the apoptotic response, ruling out nonspecific effects of heat shock or double-stranded RNA expression (Supplemental Figure S1, G–I). These results indicate that knockdown of *Cdk1* strongly represses the apoptotic response to DNA damage.

CDK1 activity is not sufficient for apoptotic competence

Together with our previous results, there were three experimental conditions that both compromised CDK1 activity and

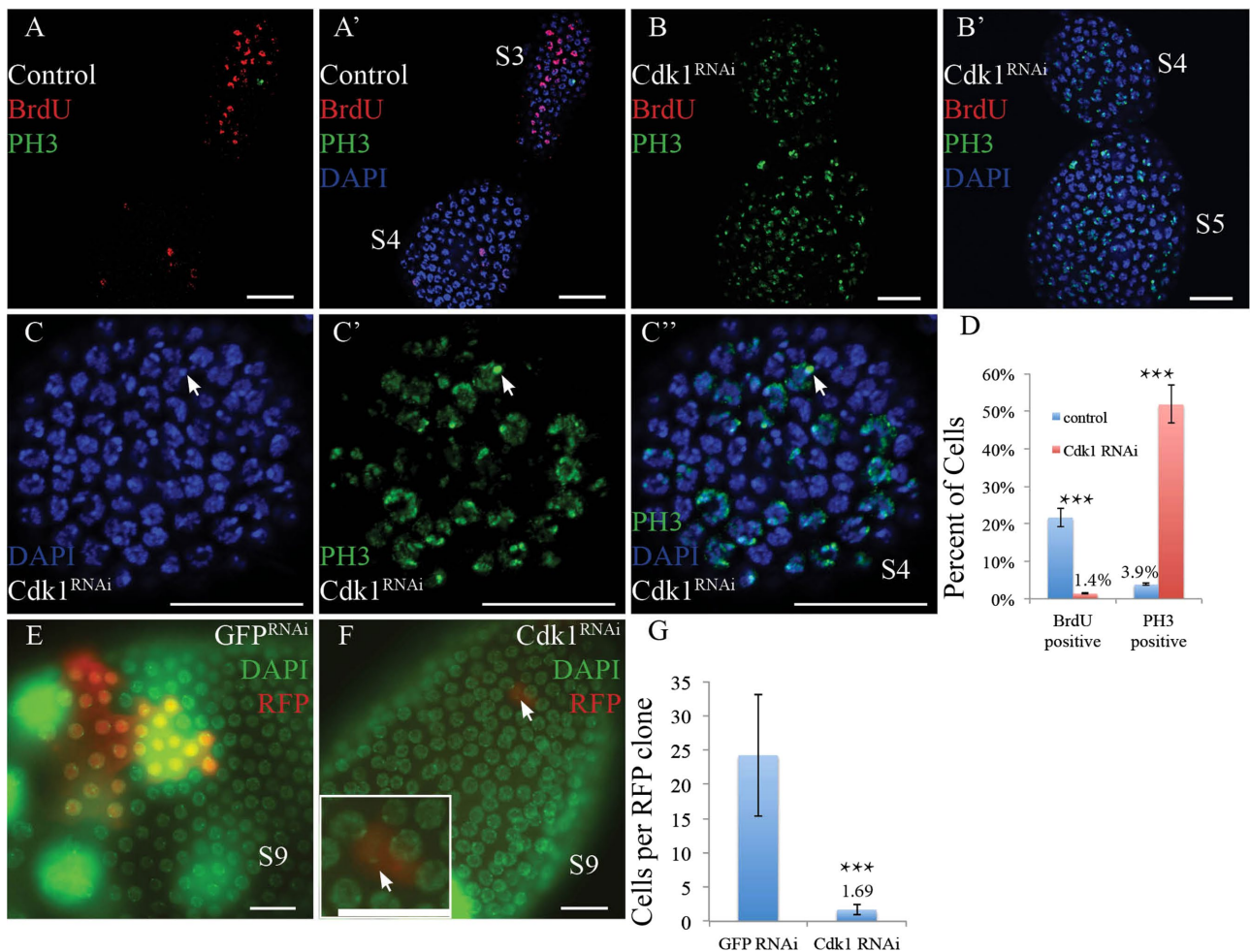


FIGURE 2: Cdk1 knockdown arrests follicle cell cycles. (A–B') Arrest of follicle cell cycles after knockdown of Cdk1. BrdU and PH3 double labeling (A, B) and triple labeling with DAPI (A', B') of *hsp70Gal4 / UAS-Cdk1^{RNAi}* stage 3–5 egg chambers without (control; A, A') or with (B, B') heat induction of Cdk1 hairpin RNA. Scale bars, 20 μ m. (C–C'') Most follicle cells are arrested at G2/M–early M phase. Higher-magnification confocal sections of PH3 labeling in a stage 4 egg chamber after Cdk1 knockdown labeled with DAPI (C), PH3 (C'), and the merge (C''). White arrow indicates one of the heterochromatic chromocenters that are intensely labeled for both DAPI and PH3. Scale bars, 20 μ m. (D) Quantification of PH3-positive and BrdU-positive follicle cells in S1–S6 egg chambers in the control or Cdk1^{RNAi} group. Mean percentages and SDs. Three biological replicates, >800 follicle cells/replicate, ****p* < 0.001 by unpaired t-test. (E, F) FLP-On clones of follicle cells expressing control *GFP^{RNAi}* (E) or *Cdk1^{RNAi}* (F) in stage 9 egg chambers 4 d after heat induction of FLP recombination. White arrow in F points to a typical one-cell RFP-positive clone that results from induction of Cdk1^{RNAi}. The same RFP-positive cell is indicated by a white arrow in the higher-magnification inset. Note that Cdk1^{RNAi} arrests the mitotic cell cycle and prevents endocycle entry and that the diploid RFP-positive cell in F has a smaller nucleus than the endocycling follicle cells outside of the clone. Scale bars, 20 μ m. (G) Quantification of the number of RFP-positive cells per clone in stage 8 and 9 egg chambers in the *GFP^{RNAi}* or Cdk1^{RNAi} groups based on 8 clones for *GFP^{RNAi}* and 36 clones for Cdk1^{RNAi} FLP-On, with *p* < 0.001 by unpaired t test.

repressed apoptosis: *Cyclin A* knockdown, *Fzr* (*Cdh1*) overexpression, and *Cdk1* knockdown (Hassel et al., 2014). Moreover, endocycling cells from many different tissue types in *Drosophila* do not have CDK1 activity or apoptose in response to IR or replication stress (Mehrotra et al., 2008; Zhang et al., 2014). These observations raised the possibility that CDK1 might directly mediate the apoptotic response to genotoxic stress. To address this idea, we tested whether misexpression of Cyclin A/CDK1 would confer apoptotic competence to endocycling cells. We used *hsp70-Gal4* to heat induce coexpression of *UAS-Cyclin A* and *UAS-Cdk1-Myc* transgenes in adult females, which resulted in high levels of Cdk1-Myc and Cyclin A proteins in mitotic cycling and endocycling follicle cells (Figure 4, A–D', and Supplemental

Figure S2; Meyer et al., 2000). Overexpression of Cyclin A/CDK1 did not change the fraction of TUNEL-positive follicle cells after IR during both mitotic cycles and endocycles. TUNEL-positive cells were frequent in mitotic cycling follicle cells of early-stage egg chambers (~10%) and were still very rare during endocycles after stage 6 ($\leq 0.1\%$; Figure 4, A–E). Therefore forced expression of Cyclin A/CDK1 does not confer apoptotic competence on endocycling follicle cells.

To test whether Cyclin A/CDK1 expression could confer an apoptotic response on other endocycling cell types, we overexpressed Cdk1 and Cyclin A in larval salivary gland cells using the *forkhead-GAL4* (*fkh-GAL4*) driver. *fkh-GAL4* expression begins at a time in mid embryogenesis when salivary gland cells switch

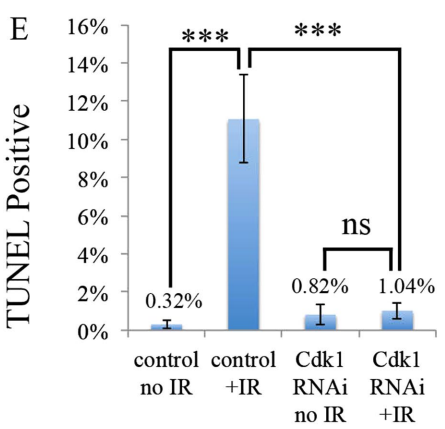
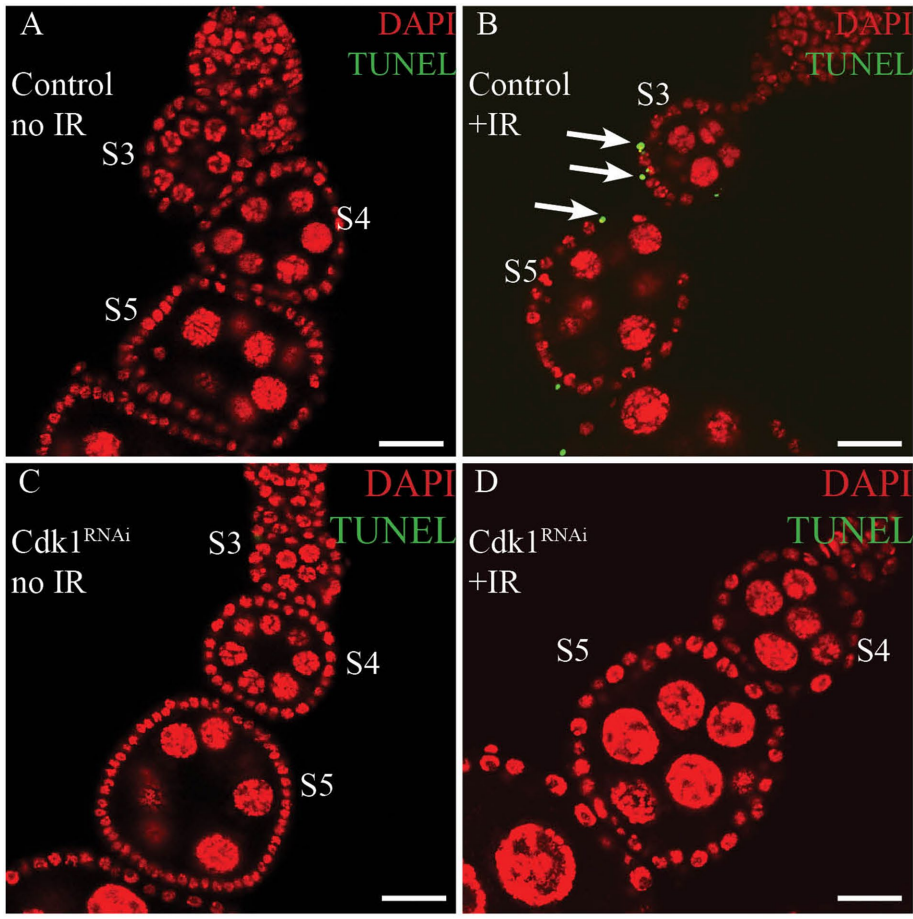


FIGURE 3: *Cdk1*-knockdown follicle cells do not apoptose in response to IR. (A–D) Double labeling for TUNEL (green) and DAPI (red) of *hsp70Gal4/UAS: Cdk1^{RNAi}* stage 3–5 egg chambers without (A, B) or with (C, D) heat-induced knockdown of *Cdk1* and without (A, C) or with (B, D) IR. White arrows in B indicate three follicle cells labeled for TUNEL. Confocal sections are through the middle of egg chambers, with epithelial follicle cells surrounding the larger nurse cells in the interior of the egg chambers. Scale bars, 20 μ m. (E) Quantification of TUNEL-positive follicle cells in stage 1–6 egg chambers in the control or *Cdk1^{RNAi}* group with or without IR. Mean percentages and SDs. Three biological replicates, >800 follicle cells/replicate, *** $p < 0.001$, not significant (ns) by unpaired t test.

from mitotic cycles to endocycles (Andrew *et al.*, 2000; Henderson and Andrew, 2000). Antibody labeling of *UAS-CycA/+; fkh-GAL4/UAS-Cdk1-myc* early third-instar larvae indicated that both CDK1-myc and Cyclin A proteins were highly expressed in salivary glands but not the adjacent fat body (Supplemental Figure S3, D–F;

unpublished data). By this stage of development, salivary gland cells normally have undergone ~10 endocycles, resulting in ~1000 copies of their genome and very large nuclei (~30 μ m; Park and Asano, 2008). In contrast, salivary gland nuclei in *CycA/CDK1*-overexpressing animals were much smaller than even the adjacent ~128–256 C polyloid fat body nuclei, which do not express *fkh-GAL4* and served as an internal control (Supplemental Figure S3, A–F; Butterworth and Rasch, 1986; Nordman *et al.*, 2011). *CycA/CDK1* overexpression in salivary gland cells strongly inhibited BrdU incorporation (0 vs. 30% in controls) and induced PH3 labeling (~70 vs. 0% in controls; Supplemental Figure S3, A–C). The small nuclear size, absence of BrdU, and strong PH3 labeling suggested that continuous misexpression of *CycA/CDK1* in salivary gland cells beginning in embryogenesis inhibited the switch to endocycles and arrested the cell cycle. Irradiation of these cells in third-instar larvae resulted in a very low frequency of TUNEL labeling that was not significantly different from that in endocycling controls (Supplemental Figure S3, D–F). Therefore similar to the result in follicle cells, expression of Cyclin A/*Cdk1* in salivary gland cells is not sufficient to confer an apoptotic response to IR.

A developmental arrest of polar follicle cells in G2 phase dampens the apoptotic response to DNA damage

Our data indicated that cells arrested in their cell cycle do not have a significant apoptotic response to DNA damage. We therefore wondered whether active mitotic cell cycling potentiates the apoptotic response to DNA damage. To further test this idea, we examined the apoptotic response of polar follicle cells (PFCs), a specialized pair of cells at each end of the egg chamber that permanently arrest in the G2 phase of the cell cycle beginning in stages 4/5 of oogenesis (Besse and Pret, 2003; Shyu *et al.*, 2009). To mark PFCs, we used a *neur^{Gal4-A101}* strain to drive *UAS-GFP* expression. We costained with antibodies against Fasciclin III (FasIII) protein, which is strongly expressed in PFCs after stage 5, which confirmed that *neur^{Gal4-A101}; UAS-GFP* uniquely marks PFCs (Figure 5, A–A’; Shyu *et al.*, 2009). After IR, the arrested PFCs had a frequency of TUNEL labeling that was significantly lower than that of proliferating main body follicle cells in the same ovariole (<2 vs. ~11%; $p = 0.0006$; Figure 5, B and C; Mehrotra *et al.*, 2008; Hassel *et al.*, 2014). These results suggest that a developmental arrest of PFCs in G2 phase of the cell cycle is associated with a dampened apoptotic response to DNA damage.

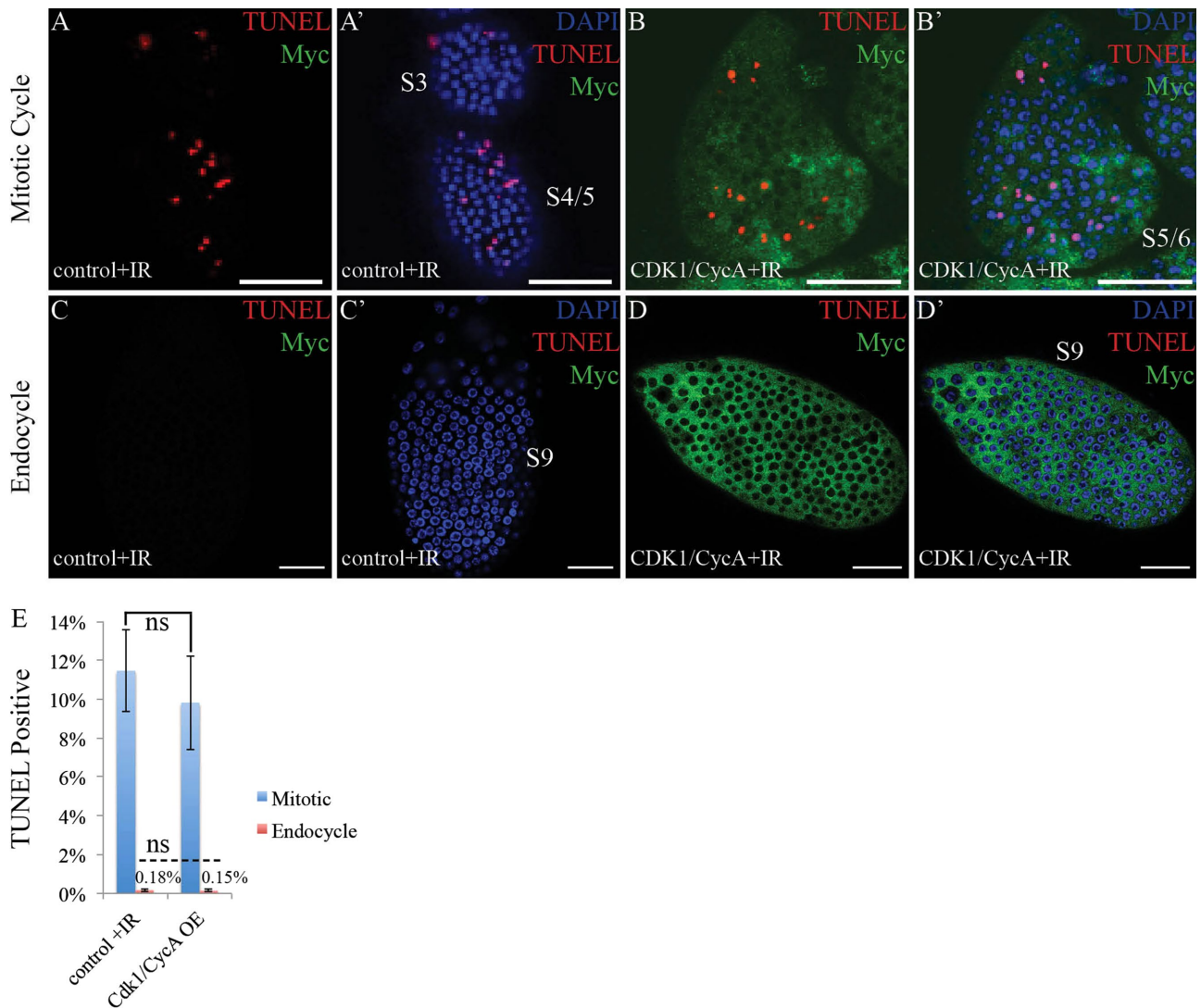


FIGURE 4: Overexpression of Cdk1/Cyclin A does not confer apoptotic competence on endocycling follicle cells. (A–B') Mitotic cycling follicle cells in early-stage egg chambers from *UAS-Cyclin A/+; hsp70Gal4/UAS-Cdk1-Myc* female after IR without (A, A') or with (B, B') heat-induced Cdk1/Cyclin A overexpression. Double labeling with anti-Myc and TUNEL (A, B) and triple labeling with DAPI (A', B'). Scale bars, 30 μ m. (C–D') Endocycling follicle cells in a stage 9 egg chamber from *UAS-Cyclin A/+; hsp70Gal4/UAS-Cdk1-Myc* female after IR without (C, C') or with (D, D') heat-induced Cdk1/Cyclin A overexpression. Double labeling for anti-Myc and TUNEL (C, D) and triple labeling with DAPI (C', D'). Scale bars, 30 μ m. (E) Quantification of TUNEL labeling in mitotic cycling (stages 1–6) and endocycling (stages 7–10A) follicle cells in control or Cdk1/Cyclin A–overexpressing females after IR. Three replicates, >800 follicle cells/replicate; ns, not significant.

Cyclin E knockdown arrests follicle cells at G1/S and represses the apoptotic response to DNA damage

The results with *Cdk1^{RNAi}* and PFCs suggested that a cell cycle arrest in G2 or early M phase is associated with a compromised apoptotic response to DNA damage. To test whether arrest at other cell cycle stages dampens apoptosis, we knocked down *Cyclin E* (*CycE*), which, together with CDK2, is required for the G1/S transition and passage through S phase (Hinds et al., 1992; Sauer and Lehner, 1995). Heat induction of a hairpin RNA of *CycE* in *hsp70-GAL4; UAS-CycE^{RNAi}* animals resulted in much lower levels of *CycE* mRNA than with controls, as evidenced by reverse transcription PCR (RT-PCR; Figure 6A). To evaluate effects of *CycE* knockdown on follicle cell cycles, we heat induced *hsp70-GAL4/UAS-CycE^{RNAi}* in the FUCCI reporter background. Knockdown of *CycE* induced a large shift in cell cycle phasing in the mitotic follicle cells before stage 6, with

almost all cells in G1/S–early S phases (Figure 6, B and C). Further analysis of the cell cycle by PH3 and BrdU double labeling showed that *CycE* knockdown resulted in a significant decrease in the number of follicle cells labeled for BrdU (<1 vs. >30% in controls) and PH3 (<1.5 vs. ~5% in controls; Figure 6, D–F). These results suggested that *Cyclin E* knockdown resulted in most mitotic follicle cells arresting at the G1/S transition, consistent with the known function of the Cyclin E/CDK2 complex. Four hours after IR, these *CycE* knockdown cells had an order-of-magnitude lower frequency of TUNEL-positive cells (<1%) than did mitotic cycling follicle cells in control animals (~10%; Figure 6, G–I). Apoptosis was also significantly lower 24 h after IR (~2 vs. ~13% in control), indicating that the delayed p53-independent apoptosis pathways are also inhibited. These results suggest that, similar to G2 or M arrest, cell cycle arrest at G1/S also severely compromises the apoptotic response to DNA damage.

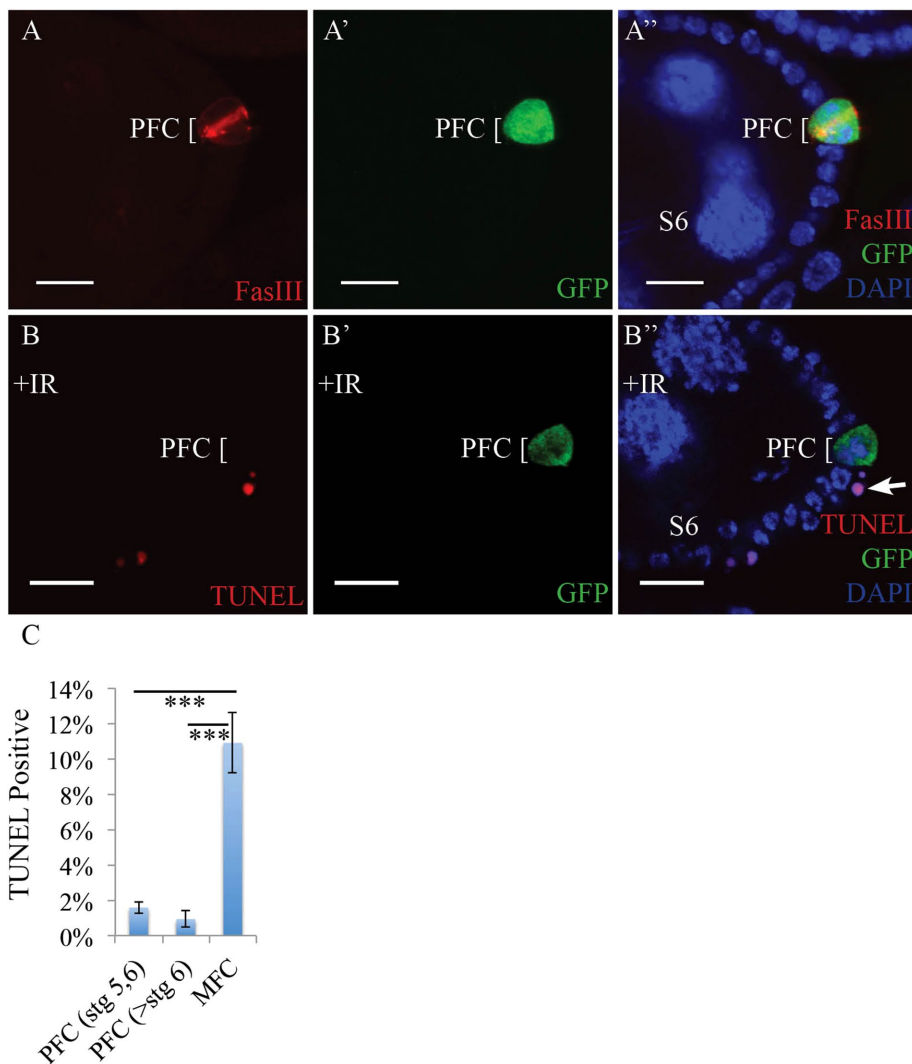


FIGURE 5: Polar follicle cells (PFCs) that are developmentally arrested in G2 phase do not apoptose after IR. FasIII (red; A), GFP (green; A'), and triple labeling with DAPI (blue; A'') of two PFCs in the posterior of a stage 6 egg chamber from a *UAS-GFP/neur^{Gal4-A101}* female without irradiation. The cell-cell contact between the two PFCs appears as a bright line of FasIII cell membrane labeling. Scale bars, 10 μ m. (B–B'') Arrested PFCs have a dampened apoptotic response to IR relative to their mitotic cycling neighbors. TUNEL (B), GFP (B'), and triple labeling with DAPI (B'') of a stage 6 egg chamber from a *UAS-GFP/neur^{Gal4-A101}* female after IR. Arrow points to one TUNEL-labeled follicle cell adjacent to the PFCs. Scale bars, 10 μ m. (C) Quantification of TUNEL-positive mitotic follicle cells (MFCs; stages 1–6) and G2/M-arrested PFCs from stage 5 and 6 and post-stage 6 egg chambers. Mean and SDs based on three replicates, >200 follicle cells/replicate, ****p* < 0.001 by unpaired *t* test.

Different cell cycle modifications can inhibit apoptosis at different steps

Our results indicated that cells arrested at different cell cycle phases, as well as actively cycling G/S endocycling cells, all have a negligible apoptotic response to DNA damage. The normal apoptotic response to DNA damage in *Drosophila* engages a phosphorylation cascade that results in activation of the *Drosophila* orthologue of the p53 tumor suppressor, which then induces transcription of several proapoptotic genes at one locus called H99 (Figure 7A). H99 genes then inhibit the *Drosophila* Inhibitor of Apoptosis Protein 1 (DIAP1), releasing DIAP1 inhibition on activator caspases (Figure 7A; Fuchs and Steller, 2011). We assayed different steps of this apoptotic pathway to determine whether different cell cycle modifications repress apoptosis in similar ways.

We began by examining one of the first steps in the apoptotic response to DNA damage—activation of the proximal checkpoint kinases ATM and ATR. These checkpoint kinases phosphorylate Chk2, which in turn phosphorylates and activates the p53 transcription factor (Figure 7A; Peters *et al.*, 2002; Fuchs and Steller, 2011). The ATM and ATR kinases also phosphorylate the histone variant H2AV at DNA damage sites (Madigan *et al.*, 2002; Joyce *et al.*, 2011). To evaluate ATM/ATR activity, therefore, we used phospho-specific antibodies against phospho-H2AV (γ -H2AV), which detects repair foci at DNA damage sites after IR (Madigan *et al.*, 2002; Lake *et al.*, 2013). Similar to control cells, both *Cdk1*- and *CycE*- knockdown cells had numerous γ -H2AV foci after IR (Figure 7, B–D). These results indicated that the apoptosis pathway is repressed downstream of ATM/ATR in *Cdk1*- and *CycE*-knockdown cells. We next examined the more downstream steps of caspase cleavage. Labeling of irradiated follicle cells with antibodies specific for the cleaved form of the effector caspase DCP-1 indicated that *Cdk1*- and *CycE*-knockdown cells have ~10-fold lower frequency of caspase cleavage than controls (~1–2 vs. 12–14% in controls), a reduction similar to that for TUNEL labeling (Figure 7, E–H; Song *et al.*, 1997; Florentin and Arama, 2012). These results suggested that the apoptotic pathway is repressed downstream of ATM activation and at or upstream of DCP-1 cleavage in *Cdk1*- and *CycE*-knockdown cell cycles. These results are similar to that for developmental endocycling cells and iECs, which we previously showed have ATM activation but a very low frequency of cleaved caspase labeling after IR (Mehrotra *et al.*, 2008; Hassel *et al.*, 2014; Zhang *et al.*, 2014).

We next evaluated whether proapoptotic H99 gene transcription was induced (Figure 7A). To assay this specifically in follicle cells, we used a reporter transgene that contains the promoter of the H99 gene *hid* fused to GFP (hereafter *hid-GFP*), which is regulated by p53 and reports the normal activation of the endogenous *hid* by radiation (Brodsky *et al.*, 2000; Tanaka-Matakatsumi *et al.*, 2009; Wichmann *et al.*, 2010; Zhang *et al.*, 2014). We previously showed that this reporter and endogenous H99 genes are not activated by IR in developmental endocycling cells, but expression in iECs was not examined (Hassel *et al.*, 2014; Zhang *et al.*, 2014). Therefore we evaluated *hid-GFP* induction after IR in iECs and compared it to *Cdk1*- and *CycE*-knockdown cells. We created iECs by knockdown of *CycA* or overexpression of *Fzr* (*Cdh1*) and measured fluorescence of anti-GFP labeling in follicle cells of stage 3–6 *hid-GFP* egg chambers. Although IR increased expression of the *hid-GFP* reporter in control mitotic cycling follicle cells, *hid-GFP* was not significantly induced in either type of iEC (Figure 8, A–D and G). These results suggest that

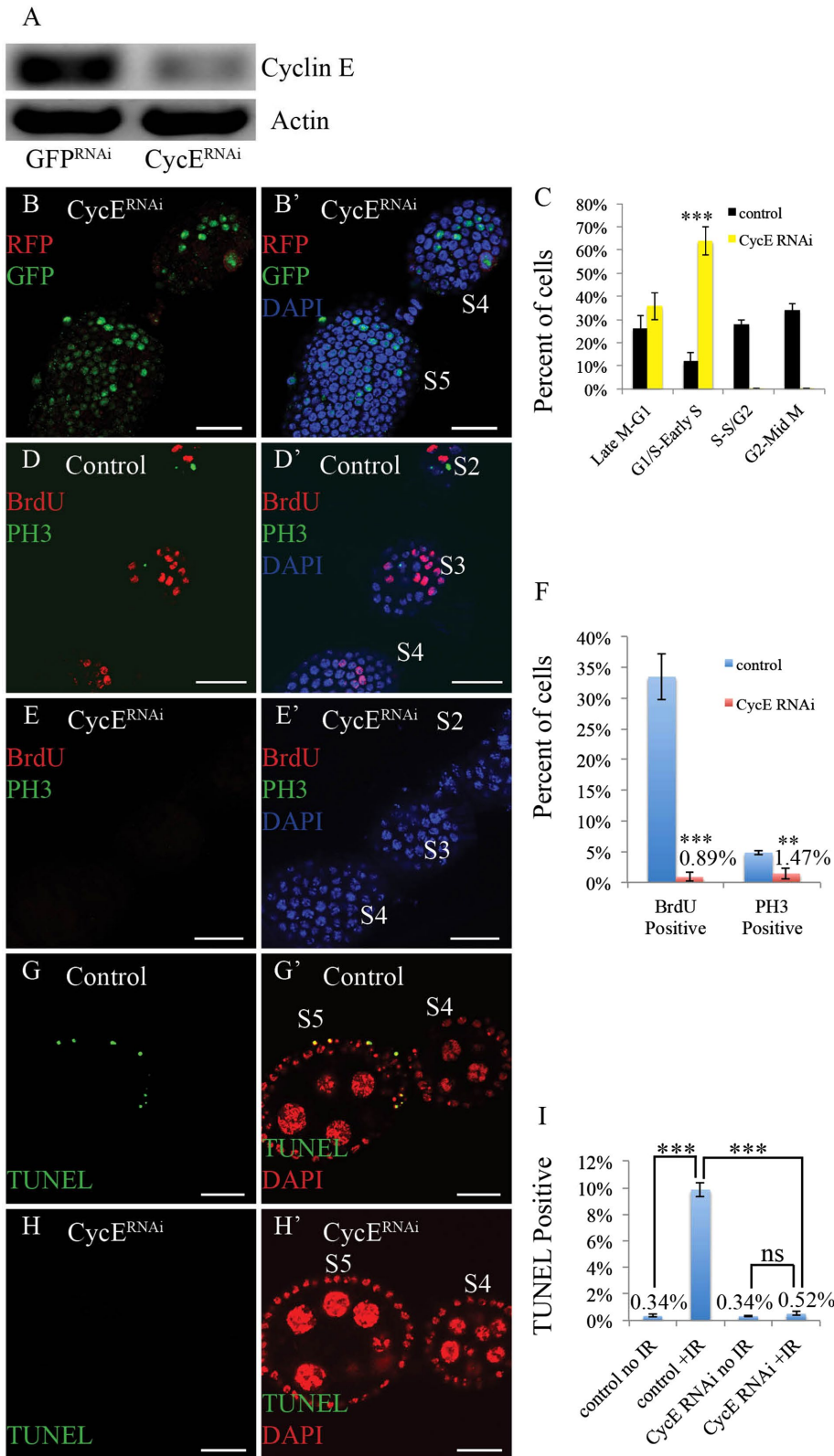


FIGURE 6: Knockdown of *Cyclin E* arrests cells at G1/S and represses apoptosis. (A) RT-PCR of actin and *Cyclin E* mRNA in *UAS-GFP^{RNAi}/+*; *hsp70-Gal4/+* and *hsp70-Gal4/UAS-CycE^{RNAi}* larvae after heat induction. (B–B') FUCCI fluorescence in *Cyclin E*-knockdown follicle cells. RFP and GFP double labeling (B) and triple labeling with DAPI (B') of *hsp70-Gal4*, *UAS-FUCCI/UAS-CycE^{RNAi}* stage 4 and 5 egg chambers after heat induction. Compare to controls in Figure 1, D and D'. Scale bars, 20 μ m. (C) Quantification of cell cycle phasing in control or *Cyclin E^{RNAi}* group based on FUCCI fluorescence. Data from Figure 1 control are replotted for comparison. Three biological replicates, >200 follicle cells/replicate, *** p < 0.001 by unpaired t test.

in both iECs and developmental endocycling cells, the apoptosis pathway is repressed upstream of *H99* gene expression. *hid-GFP* expression was also not significantly induced in *Cdk1*-knockdown cells (Figure 8, E and G). In contrast, *CycE*-knockdown cells had a strong induction of *hid-GFP* fluorescence after IR that was comparable to that for control mitotic cycling follicle cells (Figure 8, F and G). These results suggest that apoptosis is repressed upstream of *H99* gene transcription in endocycling and *Cdk1*-knockdown cells but downstream of *H99* gene transcription in *CycE*-knockdown cells. One interpretation of this result is that G1-arrested cells can induce *hid-GFP*, whereas G2- to early M-arrested cells cannot. To further address this question, we examined *hid-GFP* expression in PFCs that are developmentally arrested in G2. Like *Cdk1*-knockdown cells, PFCs had much lower levels of *hid-GFP* expression than their mitotic cycling sister cells in the same egg chamber (Figure 8, H and I). Taken together, the results suggest that different types of cell cycle modifications can repress the apoptotic response either upstream or downstream of proapoptotic *H99* gene expression.

DISCUSSION

We used the *Drosophila* ovary as a model system to investigate the coordination of cell cycles with the apoptotic response during development. We previously found that endocycling cells, both developmental and experimentally induced, do not apoptose in response to genotoxic stress (Mehrotra et al., 2008; Hassel et al., 2014; Zhang et al., 2014).

(D–E') Double labeling of BrdU and PH3 (D, E) and triple labeling with DAPI (D', E') of *hsp70-Gal4/UAS-Cdk1^{RNAi}* stage 2–4 egg chambers without (control; D, D') or with (E, E') heat-induced knockdown of *Cyclin E*. Scale bars, 20 μ m. (F) Quantification of PH3-positive and BrdU-positive follicle cells during stages 1–6 in the control or *CycE^{RNAi}* group. Three replicates, >800 follicle cells/replicate, ** p < 0.01 and *** p < 0.001 by unpaired t test. (G–H') TUNEL labeling (G, H) and double labeling with DAPI (G', H') of *hsp70-Gal4/UAS-CycE^{RNAi}* stage 4 and 5 egg chambers after IR and without (control; G, G') or with (H, H') heat-induced *CycE* knockdown. Confocal sections in G–H' are through the middle of the egg chambers. Scale bars, 20 μ m. (I) Quantification of TUNEL-positive follicle cells during stages 1–6 in the control or *CycE^{RNAi}*-knockdown groups after IR. Three replicates, >800 follicle cells/replicate, *** p < 0.001, p > 0.05, not significant (ns) by unpaired t test.

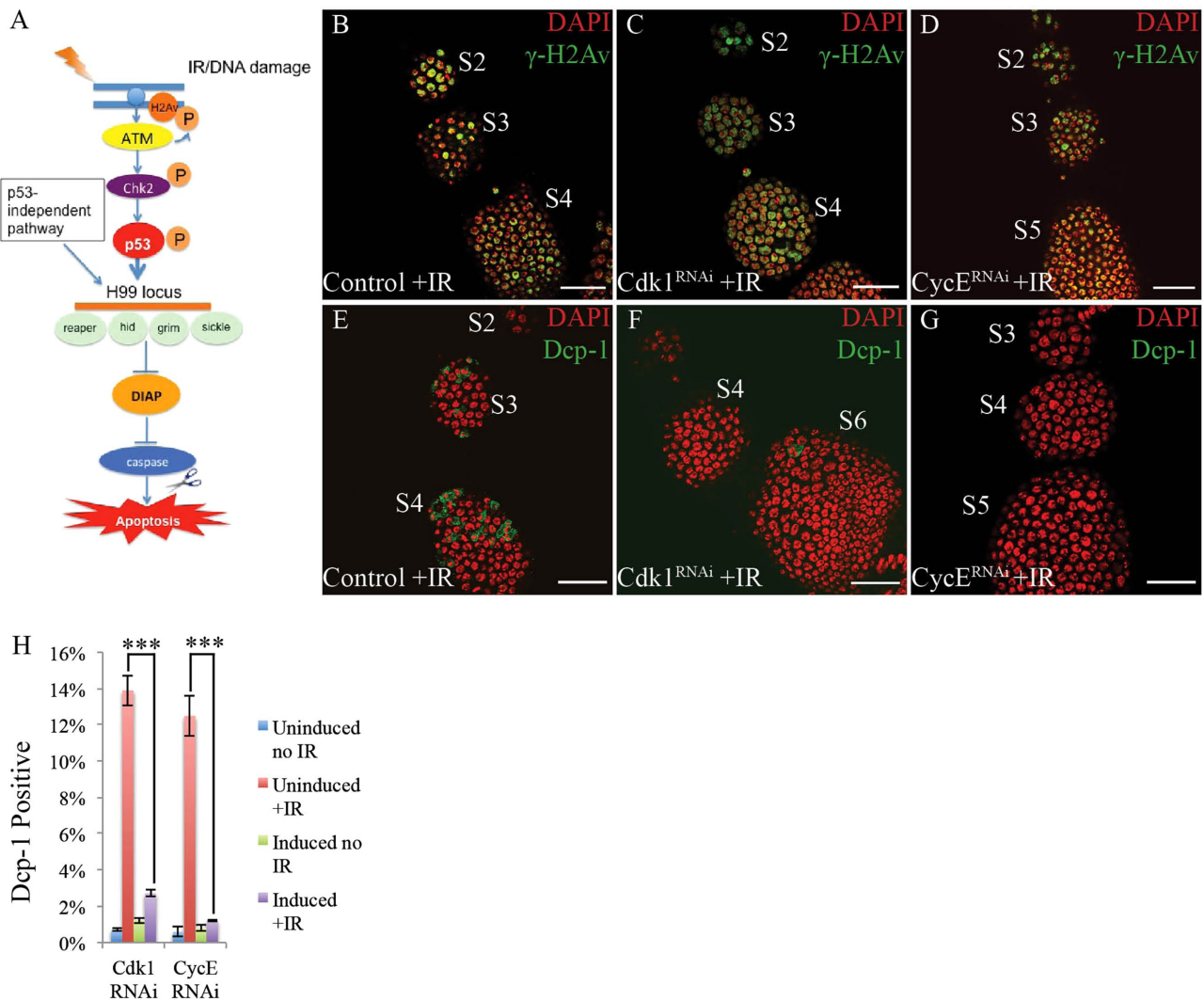


FIGURE 7: *Cdk1*- and *CycE*-knockdown cells inhibit apoptosis downstream of ATM and upstream of caspase activation. (A) The *Drosophila* DNA damage apoptotic pathway. In response to double-strand DNA breaks, ATM and ATR kinases are activated and phosphorylate several substrates, including the histone variant H2AV and the Chk2 kinase (Chk2). Activated Chk2 kinase then phosphorylates the transcription factor p53, activating it to induce expression of the proapoptotic genes at the H99 locus, *reaper*, *hid*, *grim*, and *sickle*. Expression of these H99 genes is also induced by p53-independent pathways at later time points after IR. The H99 proteins then bind and inhibit the DIAP protein, releasing DIAP's inhibition of activator caspases. The resulting caspase cleavage cascade engages a full apoptotic response. (B–D) *Cdk1*- and *CycE*-knockdown cells have active ATM/ATR. Anti-phospho H2AV (green) and DAPI (red) double labeling in irradiated control (B), *Cdk1*^{RNAi} (C), and *Cyclin E*^{RNAi} (D) follicle cells. Scale bars, 25 μ m. (E–G) Caspase cleavage is repressed in follicle cells after *Cdk1* or *CycE* knockdown. Immunolabeling for anti-cleaved caspase DCP-1 (green) and DAPI (red) in irradiated control (E), *Cdk1*-knockdown (F), and *CycE*-knockdown (G) egg chambers. Scale bars, 25 μ m. (H) Quantification of percentage of Dcp-1-positive follicle cells in S1–S6 egg chambers in *hsp70Gal4/UAS-Cdk1*^{RNAi} and *hsp70Gal4/UAS-CycE*^{RNAi} flies with or without IR. Uninduced indicates that the flies were not heat induced, and induced means that the flies were heat induced to express dsRNA for *Cdk1* or *CycE*. Three replicates, >800 follicle cells, *** $p < 0.001$.

These observations, together with those from other systems, suggested an integration of cell cycle and apoptotic pathways. Our present results indicate that arrest during different cell cycle phases also represses the apoptotic response to DNA damage independent of differentiation or developmental signals. Moreover, our data suggest that the step(s) at which the apoptosis pathway is inhibited can depend on the type of cell cycle arrest. In a broader context, our findings are relevant to understanding how cell division and the DNA damage response are coordinated during development and the ability of IR to kill cancer cells.

For several cell types and experimental conditions, low CDK1 activity correlated with reduced apoptotic response. First, *Cdk1* RNAi arrested most cells during G2/early M phase and repressed apoptosis. This cell cycle arrest is likely the result of a partial *Cdk1* knockdown because *Cdk1*-null mutations are known to induce a switch to endocycles, as does RNAi knockdown of *CycA* (Hayashi, 1996). The different strengths of *CycA* and *Cdk1* knockdown is not surprising, given that *CycA* protein is degraded each cell cycle, whereas CDK1 protein is not (Henglein *et al.*, 1994; Morgan, 1995; Yam *et al.*, 2002; Vermeulen *et al.*, 2003). Our data suggest,

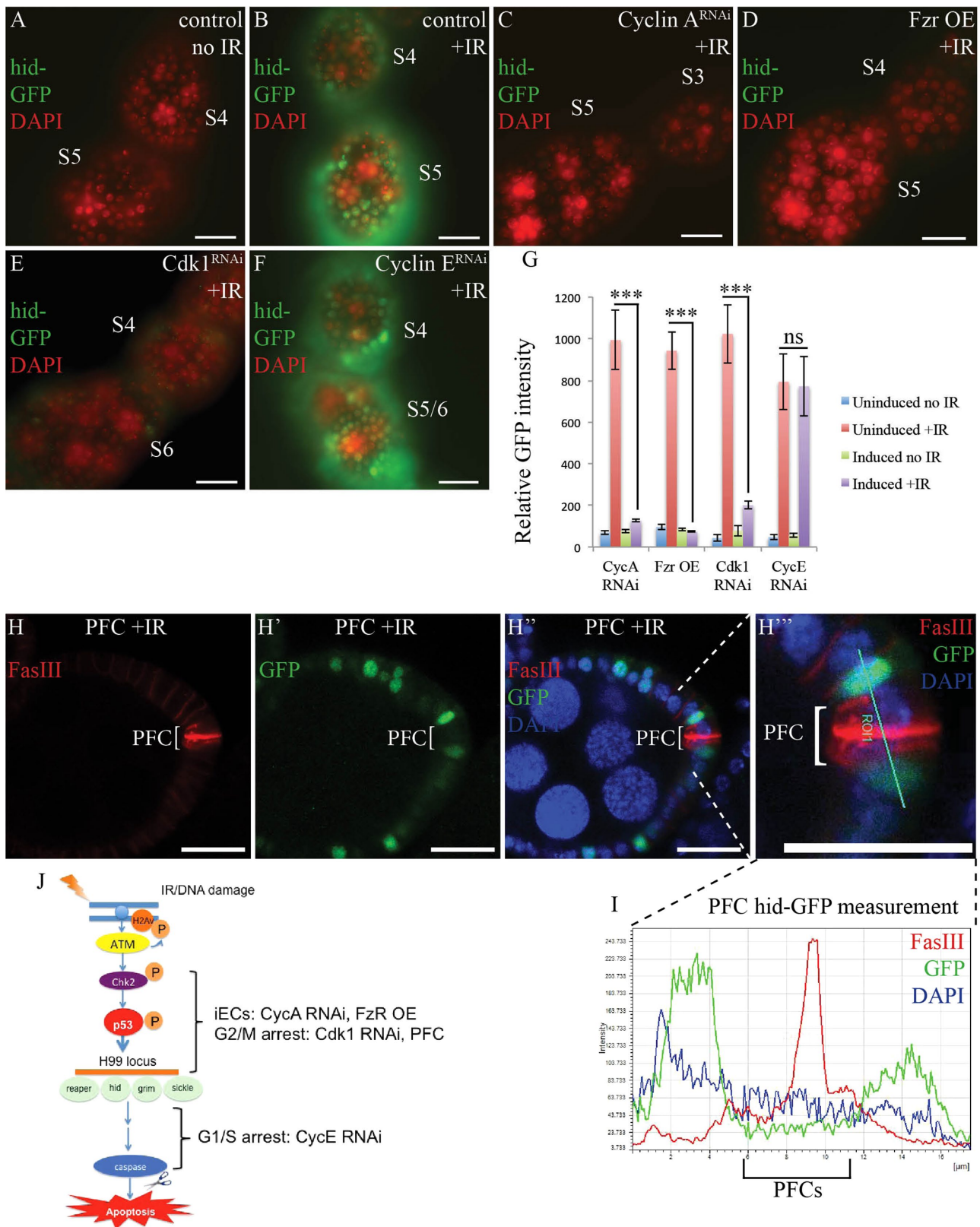


FIGURE 8: Different cell cycle modifications repress apoptosis upstream or downstream of transcription of the proapoptotic gene *hid*. (A–F) The effect of cell cycle modification on *hid-GFP* expression. (A, B) Anti-GFP detection of *hid-GFP* expression (green) in control mitotic cycling follicle cells from unirradiated (A) or irradiated (B) females. Cells were double labeled for DAPI (red). (C–F) Anti-GFP detection of *hid-GFP* expression after IR in follicle cells after knockdown of *CycA^{RNAi}* (C), *Fzr* overexpression (OE; D), *Cdk1^{RNAi}* knockdown (E), or *CycE^{RNAi}* knockdown (F). Cells were double labeled for DAPI (red). Scale bars, 20 μ m. (G) Quantification of anti-GFP fluorescence of the *hid-GFP* reporter in S1–S6 follicle cells with different cell cycle modifications. For each genotype, RNAi or overexpression (OE) was either

therefore, that most cells with low levels of CDK1 enter into but do not complete mitosis, consistent with the known functions of CDK1, and that this arrest results in a compromised apoptotic response (Morgan, 1995; Enserink and Kolodner, 2010). Second, PFCs are developmentally arrested in G2 because CDK1 is not activated by CDC25 phosphatase and have a very weak apoptotic response to IR (Shyu *et al.*, 2009). Finally, both developmental and experimentally induced endocycles lack CDK1 activity and an apoptotic response. All of these observations pointed to a possible direct requirement for CDK1 in the apoptotic response. However, resupplying CDK1/Cyclin A to endocycling cells of the ovary and salivary gland did not restore apoptotic competence, even though it had a strong inhibitory effect on endocycles. Therefore the data suggest that CDK1 activity is not sufficient and that its requirement for apoptosis is likely indirect.

Our data suggest instead that arrest at different cell cycle phases significantly reduces the apoptotic response to DNA damage (Figure 8J). The combined FUCCI and PH3 data indicated that *Cdk1* knockdown primarily arrested cells during G2-M phases, with the majority of these cells arrested during early prophase with partially condensed, PH3-labeled chromosomes. This *Cdk1* RNAi arrest reduced the frequency of apoptotic cells after IR by more than an order of magnitude. *Cyclin E* RNAi resulted in a tight cell cycle arrest at G1/S and also reduced the frequency of apoptosis by more than an order of magnitude. Moreover, the repression of apoptosis in PFCs temporally correlated with their G2/M arrest. During early stages of oogenesis, PFCs are proliferating, and a subset is culled out by developmentally induced apoptosis (Besse and Pret, 2003). The PFC cell cycle arrest is induced by Notch signaling, raising the possibility that it is the Notch pathway and not cell cycle arrest that represses apoptosis (Shyu *et al.*, 2009). Misexpression of *Cdc25* phosphatase, however, bypasses this cell cycle arrest and results in apoptosis of PFCs, consistent with the interpretation that it is cell cycle status that determines apoptotic competence (Shyu *et al.*, 2009). The evidence suggests, therefore, that active mitotic cycling is required for a full apoptotic response to DNA damage.

There are both similarities and differences among endocycling and arrested cells in their apoptotic response to DNA damage. We showed previously that endocycling cells repress apoptosis upstream of H99 gene transcription (Mehrotra *et al.*, 2008). In endocycling salivary gland cells, this is effected through proteolysis of p53 and chromatin silencing of its proapoptotic target genes at the H99 locus (Zhang *et al.*, 2014). Here, using a reporter for one of those H99 genes, *hid*, we found that induced endocycling cells also repress apoptosis upstream of *hid* transcription (Figure 8J). The G2/M-arrested PFCs and *Cdk1*-knockdown cells also did not significantly induce *hid* expression after IR, suggesting that an absence of p53-induced transcription of H99 genes also explains, at least in part, their weak apoptotic response. In contrast, although G1/S-arrested *CycE*-knockdown cells did not apoptose, *hid-GFP* was induced by IR in these cells. Thus it appears that different types of cell cycle modi-

fications repress apoptosis in different ways. Apoptosis is repressed upstream of H99 transcription in endocycling and G2/M-arrested cells, whereas it is repressed downstream of H99 transcription in G1/S-arrested cells (Figure 8J). Our data do not, however, eliminate the possibility that the apoptotic pathway is repressed at multiple steps in these cells. Indeed, this would not be surprising because cells in different developmental contexts are known to repress apoptosis using a variety of reinforcing mechanisms (Fan and Bergmann, 2014; Kang and Bashirullah, 2014; Arya and White, 2015).

Our findings are relevant to previous studies that showed that specific cells in development have an altered apoptotic response to IR. In the *Drosophila* larval wing disk, a zone of nonproliferating cells (ZNC) arrest in either G1 or G2 of the cell cycle and are resistant to IR-induced apoptosis (Johnston and Edgar, 1998; Moon *et al.*, 2005). In the larval eye disk, cells in the morphogenetic furrow transiently arrest their cell cycle in G1 and apoptose infrequently after IR (Moon *et al.*, 2008; Fan and Bergmann, 2014). Developmental signals coordinate these cell cycle arrests and can also contribute directly to the repression of apoptosis (Du *et al.*, 1996; Johnston and Edgar, 1998; Moon *et al.*, 2006; Arya and White, 2015). Our data indicate, however, that cell cycle arrest also can repress the apoptotic response independent of developmental signals. This result is consistent with previous observations from *Drosophila* and other organisms that proliferating cells tend to have a stronger apoptotic response to DNA damage than do nonproliferating cells—for example, mitotic and postmitotic neurons of the mouse brain (Hicks *et al.*, 1961; Gobbel *et al.*, 1998). Thus developmental signaling pathways and cell cycle arrest both can contribute to a dampened apoptotic response to DNA damage during development.

An important unanswered question is how cell cycle and apoptotic pathways are integrated. A cell cycle arrest at either G1/S or G2/M repressed apoptosis, suggesting that active cycling or passage through S phase may be required for a robust apoptotic response. Arguing against this interpretation is the observation that endocycling cells are in an active G/S cycle, yet also do not apoptose after IR. The one obvious shared character among all these modified cell cycles is the absence of a complete mitosis. In a variety of organisms, passage through mitosis strongly potentiates the cell death response to DNA damage, a process known as “mitotic catastrophe” (Galluzzi *et al.*, 2012; McGee, 2015). Although it is clear that mitotic catastrophe is critical for effective killing of cancer cells by radiation and other therapies, the mechanisms by which mitosis potentiates apoptosis are still being defined (Varmark *et al.*, 2009; McGee, 2015). Although the absence of mitotic progression might contribute to a dampened apoptotic response of endocycling and arrested cells, our evidence that the apoptotic pathway is blocked at different steps during G1 and G2 phases suggests that the absence of mitosis is not the only reason that apoptosis is repressed. The genetic model organism *Drosophila* represents an opportunity to further define how cell cycle and apoptotic pathways are coordinated in the context of development.

heat induced (induced) or not heat induced in sibling controls (uninduced) and were irradiated (+IR) or not irradiated (no IR). The relative *hid-GFP* fluorescence intensity on the y-axis is after background subtraction. Three biological replicates, 10 egg chambers/sample, *** $p < 0.001$ and $p > 0.05$ (ns) by unpaired *t* test. (H-I) *hid-GFP* is not induced by IR in G2/M-arrested polar follicle cells. (H-H') A confocal section through the middle of a stage 6 egg chamber from a *hid-GFP* female 4 h after irradiation. Labeling for anti-FasIII (H) and anti-GFP (H') and triple labeling with DAPI (H''). Two posterior polar follicle cells are labeled with anti-FasIII, with the cell-cell contact between them appearing as a bright line. (H''') Higher magnification of the PFCs from H. FasIII, GFP, and DAPI fluorescence intensity was quantified along the line (ROI1). Scale bars, 20 μm . (I) Quantification of fluorescence intensity along the line in H'''. The extent of the two PFCs is indicated by a bracket below the graph. (J) Model for repression of different steps of the apoptotic pathway by different cell cycle modifications.

MATERIALS AND METHODS

Drosophila genetics

Crosses were at 25°C unless otherwise noted. Most of the strains were obtained from the Bloomington *Drosophila* Stock Center (Bloomington, IN). *UAS-CycA^{RNAi}* was obtained from the Vienna *Drosophila* RNAi Center (Vienna, Austria), and *UAS-fzr-III* was provided by C. Lehner (University of Zurich; Sigrist and Lehner, 1997). FUCCI strains were a generous gift from Bruce Edgar's lab (University of Heidelberg; Zielke *et al.*, 2014). The *hid-GFP* fly strain was provided by W. Du (University of Chicago; Tanaka-Matakatsu *et al.*, 2009). *hsp70-Gal4*, *hid-GFP* flies were crossed to different UAS strains to assess *hid* reporter activity during modified cell cycles. *UAS-FUCCI*; *hsp70-Gal4* strain and *UAS-CycA*; *UAS-Cdk1-Myc* strain were generated by genetic crosses. For all heat-inducible RNAi or overexpression experiments, larvae or adult flies were heat treated at 37°C for 30 min multiple times. *CycE* RNAi and *Fzr* overexpression was induced by heat pulsing twice per day for a total five heat pulses, and *Cdk1* RNAi and *CycA* RNAi were induced twice a day for a total of seven heat pulses. Overexpression of *Cdk1* and *CycA* in salivary glands or follicle cells was induced by one heat pulse. *FLP-On* clones were created in *hsp70-FLPase/+*; *Actin <CD2>GAL4 UAS-RFP/UAS-Cdk1^{RNAi}* (or *UAS-GFP^{RNAi}*) females by one 45-min heat induction at 37°C, and the RFP clone size was analyzed in stage 8/9 egg chambers 4 d later (Pignoni and Zipursky, 1997).

RNA isolation and semiquantitative RT-PCR

Total RNA was isolated from whole larvae using TRIzol (15596-026; Invitrogen, Waltham, MA). We reverse transcribed 1 mg of RNA from each sample using Superscript III First Strand (Invitrogen) according to the manufacturer's instructions. The same amount of cDNA from each sample was amplified by PCR using primers spanning introns of *Cdk1* or *CycE*, with primers to *Actin* 5C used as a control. The resulting products were analyzed by standard agarose gel electrophoresis.

Immunofluorescence microscopy and quantification

Ovaries were fixed and labeled as previously described (Schwed *et al.*, 2002), using the following antibodies and concentrations: rabbit anti-phospho-histone H3 (PH3), 1:200 (Millipore, Billerica, MA); mouse anti-phospho-histone H3 (PH3), 1:100 (Cell Signaling, Danvers, MA); mouse anti-Cyclin A, 1:100 (Developmental Studies Hybridoma Bank [DSHB], University of Iowa, Iowa City, IA); mouse anti-Myc, 1:50 (DSHB); rabbit anti-GFP, 1:500 (Invitrogen); mouse anti- γ H2Av (1:8000; a gift from J. Sekelsky [University of North Carolina] and S. Hawley [Stowers Institute]; Lake *et al.*, 2013); rabbit anti-Dcp-1, 1:100 (Cell Signaling); and mouse anti-FasIII, 1:15 (DSHB). BrdU incorporation was for 1 h in vitro, and anti-BrdU labeling was as previously described (Calvi and Lilly, 2004). Micrographs were taken on a Leica DMRA2 wide-field microscope or a Leica SP5 confocal. For measurements of labeling frequencies, follicle cells were counted in multiple ovarioles over at least three biological replicates, and significance relative to parallel controls was calculated by an unpaired Student's *t* test. The intensity of *hid-GFP* fluorescence in Figure 8 was quantified in wide field using Openlab (Improvision, Coventry, England) by measuring the mean pixel fluorescence intensity of randomly chosen egg chambers. These mean values were then background subtracted using pixels in the same image. The Leica SP5 quantification software package was used to quantify the fluorescence intensity of *hid-GFP* in PFC's in Figure 8, H–H''.

γ -Irradiation

Flies were irradiated with a total of 40 Gy from a cesium source and labeled with anti-Dcp-1 (Cell Signaling), anti- γ H2Av, or TUNEL (In Situ Cell Death Detection Kit, TMR red, version 11 (12 156 792 910; Roche, Basel, Switzerland) either 4 or 24 h after irradiation.

ACKNOWLEDGMENTS

We thank the Bloomington *Drosophila* Stock Center, M. Lilly, B. Edgar, and W. Du for fly strains and J. Sekelsky and S. Hawley for antibodies. We also thank J. Powers of the Indiana Light Microscopy Imaging Center for technical support and advice and M. Rotelli and C. Walczak for helpful comments on the manuscript. This research was supported by National Institutes of Health Grant R01GM113107 to B.R.C. and the Indiana Clinical and Translational Sciences Institute, Indiana University, which is funded in part by Grant UL1 TR001108 from the National Institutes of Health, National Center for Advancing Translational Sciences, Clinical and Translational Sciences Award.

REFERENCES

- Andrew DJ, Henderson KD, Seshiah P (2000). Salivary gland development in *Drosophila melanogaster*. *Mech Dev* 92, 5–17.
- Arya R, White K (2015). Cell death in development: signaling pathways and core mechanisms. *Semin Cell Dev Biol* 39, 12–19.
- Baldwin WF, Salthouse TN (1959). Latent radiation damage and synchronous cell division in the epidermis of an insect. I. Nonreversible effects leading to local radiation burns. *Radiat Res* 10, 387–396.
- Besse F, Pret AM (2003). Apoptosis-mediated cell death within the ovarian polar cell lineage of *Drosophila melanogaster*. *Development* 130, 1017–1027.
- Brodsky MH, Nordstrom W, Tsang G, Kwan E, Rubin GM, Abrams JM (2000). *Drosophila* p53 binds a damage response element at the reaper locus. *Cell* 101, 103–113.
- Butterworth FM, Rasch EM (1986). Adipose tissue of *Drosophila melanogaster*: VII. Distribution of nuclear DNA amounts along the anterior-posterior axis in the larval fat body. *J Exp Zool* 239, 77–85.
- Calvi BR (2006). Developmental DNA amplification. In: *DNA Replication and Human Disease*, ed. ML DePamphilis, Cold Spring Harbor, NY: Cold Spring Harbor Laboratory Press, 233–255.
- Calvi BR (2013). Making big cells: one size does not fit all. *Proc Natl Acad Sci USA* 110, 9621–9622.
- Calvi BR, Lilly MA (2004). BrdU labeling and nuclear flow sorting of the *Drosophila* ovary. In: *Drosophila Cytogenetics Protocols*, ed. D Henderson, Totowa, NJ: Humana Press, 203–213.
- Ciccia A, Elledge SJ (2010). The DNA damage response: making it safe to play with knives. *Mol Cell* 40, 179–204.
- Du W, Xie JE, Dyson N (1996). Ectopic expression of dE2F and dDP induces cell proliferation and death in the *Drosophila* eye. *EMBO J* 15, 3684–3692.
- Enserink JM, Kolodner RD (2010). An overview of Cdk1-controlled targets and processes. *Cell Div* 5, 11.
- Fan Y, Bergmann A (2008). Distinct mechanisms of apoptosis-induced compensatory proliferation in proliferating and differentiating tissues in the *Drosophila* eye. *Dev Cell* 14, 399–410.
- Fan Y, Bergmann A (2014). Multiple mechanisms modulate distinct cellular susceptibilities toward apoptosis in the developing *Drosophila* eye. *Dev Cell* 30, 48–60.
- Florentin A, Arama E (2012). Caspase levels and execution efficiencies determine the apoptotic potential of the cell. *J Cell Biol* 196, 513–527.
- Fox DT, Duronio RJ (2013). Endoreplication and polyploidy: insights into development and disease. *Development* 140, 3–12.
- Fuchs Y, Steller H (2011). Programmed cell death in animal development and disease. *Cell* 147, 742–758.
- Galluzzi L, Vitale I, Abrams JM, Alnemri ES, Baehrecke EH, Blagosklonny MV, Dawson TM, Dawson VL, El-Deiry WS, Fulda S, *et al.* (2012). Molecular definitions of cell death subroutines: recommendations of the Nomenclature Committee on Cell Death 2012. *Cell Death Differ* 19, 107–120.
- Gavrieli Y, Sherman Y, Ben-Sasson SA (1992). Identification of programmed cell death in situ via specific labeling of nuclear DNA fragmentation. *J Cell Biol* 119, 493–501.

- Gobbel GT, Bellinzona M, Vogt AR, Gupta N, Fike JR, Chan PH (1998). Response of postmitotic neurons to X-irradiation: implications for the role of DNA damage in neuronal apoptosis. *J Neurosci* 18, 147–155.
- Hanahan D, Weinberg RA (2011). Hallmarks of cancer: the next generation. *Cell* 144, 646–674.
- Hassel C, Zhang B, Dixon M, Calvi BR (2014). Induction of endocycles represses apoptosis independently of differentiation and predisposes cells to genome instability. *Development* 141, 112–123.
- Hayashi S (1996). A Cdc2 dependent checkpoint maintains diploidy in *Drosophila*. *Development* 122, 1051–1058.
- Henderson KD, Andrew DJ (2000). Regulation and function of Scr, exd, and hth in the *Drosophila* salivary gland. *Dev Biol* 217, 362–374.
- Hendzel MJ, Wei Y, Mancini MA, Van Hooser A, Ranalli T, Brinkley BR, Bazett-Jones DP, Allis CD (1997). Mitosis-specific phosphorylation of histone H3 initiates primarily within pericentromeric heterochromatin during G2 and spreads in an ordered fashion coincident with mitotic chromosome condensation. *Chromosoma* 106, 348–360.
- Henglein B, Chenivesse X, Wang J, Eick D, Brecht C (1994). Structure and cell cycle-regulated transcription of the human cyclin A gene. *Proc Natl Acad Sci USA* 91, 5490–5494.
- Hicks SP, D'Amato CJ, Coy MA, O'Brien ED, Thurston JM, Joftes DL (1961). Migrating cells in the developing nervous system studied by their radiosensitivity and tritiated thymidine uptake. *Brookhaven Symp Biol* 14, 246–261.
- Hinds PW, Mittnacht S, Dulic V, Arnold A, Reed SI, Weinberg RA (1992). Regulation of retinoblastoma protein functions by ectopic expression of human cyclins. *Cell* 70, 993–1006.
- Hudson AM, Cooley L (2014). Methods for studying oogenesis. *Methods* 68, 207–217.
- Jackson JG, Post SM, Lozano G (2011). Regulation of tissue- and stimulus-specific cell fate decisions by p53 in vivo. *J Pathol* 223, 127–136.
- Johnston LA, Edgar BA (1998). Wingless and Notch regulate cell-cycle arrest in the developing *Drosophila* wing. *Nature* 394, 82–84.
- Joyce EF, Pedersen M, Tiong S, White-Brown SK, Paul A, Campbell SD, McKim KS (2011). *Drosophila* ATM and ATR have distinct activities in the regulation of meiotic DNA damage and repair. *J Cell Biol* 195, 359–367.
- Kang Y, Bashirullah A (2014). A steroid-controlled global switch in sensitivity to apoptosis during *Drosophila* development. *Dev Biol* 386, 34–41.
- Klusza S, Deng WM (2011). At the crossroads of differentiation and proliferation: precise control of cell-cycle changes by multiple signaling pathways in *Drosophila* follicle cells. *Bioessays* 33, 124–134.
- Lake CM, Korda Holsclaw J, Bellendir SP, Sekelsky J, Hawley RS (2013). The development of a monoclonal antibody recognizing the *Drosophila* melanogaster phosphorylated histone H2A variant (gamma-H2AV). *G3 (Bethesda)* 3, 1539–1543.
- Leslie M (2014). Strength in numbers? *Science* 343, 725–727.
- Madigan JP, Chotkowski HL, Glaser RL (2002). DNA double-strand break-induced phosphorylation of *Drosophila* histone variant H2Av helps prevent radiation-induced apoptosis. *Nucleic Acids Res* 30, 3698–3705.
- McGee MM (2015). Targeting the mitotic catastrophe signaling pathway in cancer. *Mediators Inflamm* 2015, 146282.
- Mehrotra S, Maqbool SB, Kolpakas A, Murnen K, Calvi BR (2008). Endocycling cells do not apoptose in response to DNA rereplication genotoxic stress. *Genes Dev* 22, 3158–3171.
- Meyer CA, Jacobs HW, Datar SA, Du W, Edgar BA, Lehner CF (2000). *Drosophila* Cdk4 is required for normal growth and is dispensable for cell cycle progression. *EMBO J* 19, 4533–4542.
- Mihaylov IS, Kondo T, Jones L, Ryzhikov S, Tanaka J, Zheng J, Higa LA, Minamino N, Cooley L, Zhang H (2002). Control of DNA replication and chromosome ploidy by geminin and cyclin A. *Mol Cell Biol* 22, 1868–1880.
- Moon NS, Di Stefano L, Dyson N (2006). A gradient of epidermal growth factor receptor signaling determines the sensitivity of rbf1 mutant cells to E2F-dependent apoptosis. *Mol Cell Biol* 26, 7601–7615.
- Moon NS, Di Stefano L, Morris EJ, Patel R, White K, Dyson NJ (2008). E2F and p53 induce apoptosis independently during *Drosophila* development but intersect in the context of DNA damage. *PLoS Genet* 4, e1000153.
- Moon NS, Frolov MV, Kwon EJ, Di Stefano L, Dimova DK, Morris EJ, Taylor-Harding B, White K, Dyson NJ (2005). *Drosophila* E2F1 has context-specific pro- and antiapoptotic properties during development. *Dev Cell* 9, 463–475.
- Morgan DO (1995). Principles of CDK regulation. *Nature* 374, 131–134.
- Ni JQ, Liu LP, Binari R, Hardy R, Shim HS, Cavallaro A, Booker M, Pfeiffer BD, Markstein M, Wang H, et al. (2009). A *Drosophila* resource of transgenic RNAi lines for neurogenetics. *Genetics* 182, 1089–1100.
- Nordman J, Li S, Eng T, Macalpine D, Orr-Weaver TL (2011). Developmental control of the DNA replication and transcription programs. *Genome Res* 21, 175–181.
- Ollmann M, Young LM, Di Como CJ, Karim F, Belvin M, Robertson S, Whittaker K, Demsky M, Fisher WW, Buchman A, et al. (2000). *Drosophila* p53 is a structural and functional homolog of the tumor suppressor p53. *Cell* 101, 91–101.
- Park SY, Asano M (2008). The origin recognition complex is dispensable for endoreplication in *Drosophila*. *Proc Natl Acad Sci USA* 105, 12343–12348.
- Peters M, DeLuca C, Hirao A, Stambolic V, Potter J, Zhou L, Liepa J, Snow B, Arya S, Wong J, et al. (2002). Chk2 regulates irradiation-induced, p53-mediated apoptosis in *Drosophila*. *Proc Natl Acad Sci USA* 99, 11305–11310.
- Pignoni F, Zipursky SL (1997). Induction of *Drosophila* eye development by decapentaplegic. *Development* 124, 271–278.
- Sakaue-Sawano A, Kurokawa H, Morimura T, Hanyu A, Hama H, Osawa H, Kashiwagi S, Fukami K, Miyata T, Miyoshi H, et al. (2008). Visualizing spatiotemporal dynamics of multicellular cell-cycle progression. *Cell* 132, 487–498.
- Sauer K, Knoblich JA, Richardson H, Lehner CF (1995). Distinct modes of cyclin E/cdc2c kinase regulation and S-phase control in mitotic and endoreduplication cycles of *Drosophila* embryogenesis. *Genes Dev* 9, 1327–1339.
- Sauer K, Lehner CF (1995). The role of cyclin E in the regulation of entry into S phase. *Prog Cell Cycle Res* 1, 125–139.
- Schwed G, May N, Pechersky Y, Calvi BR (2002). *Drosophila* minichromosome maintenance 6 is required for chorion gene amplification and genomic replication. *Mol Biol Cell* 13, 607–620.
- Shyu LF, Sun J, Chung HM, Huang YC, Deng WM (2009). Notch signaling and developmental cell-cycle arrest in *Drosophila* polar follicle cells. *Mol Biol Cell* 20, 5064–5073.
- Sigrist SJ, Lehner CF (1997). *Drosophila* fizzy-related down-regulates mitotic cyclins and is required for cell proliferation arrest and entry into endocycles. *Cell* 90, 671–681.
- Song Z, McCall K, Steller H (1997). DCP-1, a *Drosophila* cell death protease essential for development. *Science* 275, 536–540.
- Spear FG, Glucksmann A (1941). The effect of gamma radiation on cells in vivo. Part III. Spaced radiation. *Br J Radiol* 14, 65–76.
- Spradling AC (1993). Developmental genetics of oogenesis. In: *The Development of Drosophila melanogaster*, ed. M Bate and A Martinez-Arias, Cold Spring Harbor, NY: Cold Spring Harbor Laboratory Press, 1–70.
- Tanaka-Matakatsu M, Xu J, Cheng L, Du W (2009). Regulation of apoptosis of rbf mutant cells during *Drosophila* development. *Dev Biol* 326, 347–356.
- Varmark H, Sparks CA, Nordberg JJ, Koppetsch BS, Theurkauf WE (2009). DNA damage-induced cell death is enhanced by progression through mitosis. *Cell Cycle* 8, 2951–2963.
- Vermeulen K, Van Bockstaele DR, Berneman ZN (2003). The cell cycle: a review of regulation, deregulation and therapeutic targets in cancer. *Cell Prolif* 36, 131–149.
- Weinert TA, Hartwell LH (1993). Cell cycle arrest of cdc mutants and specificity of the RAD9 checkpoint. *Genetics* 134, 63–80.
- Wichmann A, Jaklevic B, Su TT (2006). Ionizing radiation induces caspase-dependent but Chk2- and p53-independent cell death in *Drosophila* melanogaster. *Proc Natl Acad Sci USA* 103, 9952–9957.
- Wichmann A, Uyetake L, Su TT (2010). E2F1 and E2F2 have opposite effects on radiation-induced p53-independent apoptosis in *Drosophila*. *Dev Biol* 346, 80–89.
- Yam CH, Fung TK, Poon RY (2002). Cyclin A in cell cycle control and cancer. *Cell Mol Life Sci* 59, 1317–1326.
- Zhang B, Mehrotra S, Ng WL, Calvi BR (2014). Low levels of p53 protein and chromatin silencing of p53 target genes repress apoptosis in *Drosophila* endocycling cells. *PLoS Genet* 10, e1004581.
- Zielke N, Korzelius J, van Straaten M, Bender K, Schuhknecht GF, Dutta D, Xiang J, Edgar BA (2014). Fly-FUCCI: a versatile tool for studying cell proliferation in complex tissues. *Cell Rep* 7, 588–598.